Nucleic Acids Research, Vol. 20, No. 18 4727–4731

A new approach to the analysis of DNase I footprinting data and its application to the TFIIIA/5S DNA complex

Louise Fairall and Daniela Rhodes
MRC Laboratory of Molecular Biology, Hills Road, Cambridge CB2 2QH, UK

Received July 17, 1992; Revised and Accepted August 17, 1992

ABSTRACT

We have re-examined DNase I footprinting data for the binding of transcription factor IIIA (TFIIIA) to the 5S RNA gene, taking into account the protein-DNA contacts observed in the crystal structure of the DNase I/DNA complex (1, 2). This structure was not available when many of the original footprinting experiments on the TFIIIA/DNA complex were performed. In this way the pattern of DNase I cleavage can be interpreted to map out with greater precision the regions on the 5S DNA occupied by TFIIIA. Then, assuming the binding site for a zinc-finger may be the same as that found in the structure of the zinc-finger protein Zif268/DNA complex (3), and taking into account footprinting data for truncated forms of TFIIIA, the TFIIIA zinc-fingers were fitted within the permitted regions. On the basis of this, an alignment of the zinc-fingers of TFIIIA with its DNA binding site is proposed, which combines features of earlier models (4).

INTRODUCTION

The transcription factor IIIA (TFIIIA) regulates the transcription of 5S RNA genes in *Xenopus laevis*. The DNA-binding mini-domain, now termed zinc-finger, was first observed in TFIIIA where it is repeated nine times in tandem (5). Since that time it has become clear that the zinc-finger is the most widespread DNA-binding motif discovered so far and has been found in the sequences of over 200 proteins (6). This zinc-finger motif consists of 30 amino acids folded around a central zinc ion to form an independent mini-domain. The consensus sequence of the zinc-finger motif is Ψ-x-C-x_{2-4}-C-x_3-Ψ-x_5-Ψ-x_2-H-x_{3-4}-H-x_5 (where Ψ represents a large hydrophobic amino acid and x any amino acid). Unlike other DNA-binding motifs, zinc-fingers are almost always repeated within a single protein and are arranged head to tail repeated from 2 to 37 times. It has emerged from biochemical studies that zinc-fingers are used as modules for the building up of the DNA-binding domains of various proteins (7–13). Given this modular design for sequence-specific recognition and the wide occurrence of the zinc-finger motif, it is clearly of general importance to understand how zinc-fingers are used in binding to DNA and in particular, whether there is a general mechanism for binding.

Several years ago we began a study to understand how the nine zinc-fingers of TFIIIA bind to the 50 base-pair target binding site within the 5S RNA gene. Given the repeated nature of the protein we expected that the protein would bind to DNA by making multiple repeated contacts (14). It seemed that there were two possible regular geometries for this binding (termed models I and II). In model I the protein would spiral continuously around the major groove with every finger making equivalent contacts 5 bp apart. In model II the protein lies along one face of the double helix with pairs of fingers binding in the major groove and alternate linkers between fingers crossing the minor groove. We carried out a comprehensive footprinting study using a number of nucleases and chemical reagents (4, 15), giving results which, on the assumption of regularly repeated contacts, were only consistent with model II. Thus we proposed that on average each zinc-finger binds to about 5 bp in the major groove of DNA, and the protein as a whole lies on one face of the DNA double helix. A more detailed model of this type was later proposed by Churchill *et al.* on the basis of further data from hydroxyl radical footprinting studies (16).

A less regular model has been proposed by Berg (17). In this model the first five fingers (fingers 1–5) follow each other in the major groove of the DNA, in a similar manner to the fingers in the Zif268-DNA complex. The next finger, finger 6, is used to span a whole turn of the DNA double helix, and in order to accommodate this, the DNA is bent in this region. Then fingers 7, 8 and 9 follow each other again in the major groove. In this model the fingers are oriented so that finger 9 binds to the 5′ end of the binding site as shown by Smith *et al.* (7).

More recently the results of two crystal structure determinations have stimulated us to examine the footprinting data for TFIIIA anew. The first is the structure of the complex between the zinc-finger protein Zif268 and DNA (3). This gives us a direct insight into how, in a particular case, zinc-fingers bind to DNA in a sequence specific manner. In this structure the three zinc-fingers of Zif268 follow each other in the major groove for almost a complete turn of the DNA helix, each finger making equivalent contacts to one of the two DNA strands. However, there is no simple way of explaining all the footprinting data for TFIIIA in terms of the continuous mode of binding seen in the structure of the Zif268/DNA complex. The second structure is that of a DNase I/DNA complex, which shows in detail the DNA binding site for the enzyme (1, 2). This structure permits the interpretation of DNase I footprints with more precision than was previously possible (13) and we have applied it here to deduce the regions within the whole DNase I footprint occupied by TFIIIA. With

these new pieces of structural information we have been able to fit the nine zinc-fingers of TFIIIA within its 50 base pair binding site.

Mapping the DNA binding site for TFIIIA using results from the structure of the DNase I/DNA complex

The nuclease DNase I has been used extensively to study the interaction of DNA-binding proteins with their binding sites. Until recently it was difficult to define at high resolution the binding sites of a protein using a DNase I footprint, because the cleavage mechanism of the enzyme was not well understood. The crystal structure of the DNase I/DNA complex provides an understanding of the structural requirements for DNase I to cleave DNA (1, 2) and consequently a concrete basis for interpreting DNase I footprinting data (13). DNase I binds to the minor groove of DNA and cleaves each strand independently. The binding site, which is occupied by DNase I when it cleaves the phosphate backbone at one position, is shown schematically in Figure 1a. The nuclease binds asymmetrically to the minor groove of DNA covering the whole of the major groove in the region of the cleavage site. It contacts two phosphates on each side of the cleaved bond and two phosphates on the other strand across the minor groove, opposite the phosphates contacted on the 5′ side of the cleaved bond. With this information at hand we have re-examined the DNase I footprinting data for TFIIIA.

When TFIIIA is bound to a 5S RNA gene it protects about 50 bp (the internal control region) from DNase I cleavage: nucleotides 45 to 97 on the non-coding strand and nucleotides 45 to 95 on the coding strand. Whilst the coding strand is almost entirely protected within the binding site (see legend to Figure 2), it is striking that on the non-coding strand there are two short regions of DNA which are cleaved by DNase I with high frequency. These internal cleavage sites span several bonds and are located at nucleotides 60 to 63 and 73 to 76 on the non-coding strand (15, 18, 19). The fact that the cleavage sites coincide, approximately, with the structural periodicity of double helical DNA (i.e. the minor groove is exposed at positions centred on nucleotides 42, 62, 74 and 93) indicated to us that the protein as a whole is likely to bind to one side of the DNA double helix (4). It is also likely that TFIIIA distorts the DNA because the cleavage sites located nucleotides 60–63 are not cut in the naked DNA. In Figure 2 we have plotted, on a cylindrical projection of the DNA double helix, the DNase I cleavage sites that define the borders of the footprint, and the strong internal cleavage sites on the non-coding strand. The contacts (Figure 1a) that must be made by DNase I with the DNA to make these observed cleavages are also shown in the plot. (Since footprinting is carried out under conditions where there is only about one cut per DNA molecule, each arrow in Figure 2 represents an independent cut. Therefore where there are adjacent cuts the DNase I binding sites overlap.) In this way it can be seen that the comparatively large extent of DNA required for DNase I to bind and cleave at the observed sites correspondingly reduces the area within the whole protected region that may be occupied by TFIIIA. Subtraction of the area occupied by DNase I at each cleavage site leaves three patches of DNA available for TFIIIA binding: from nucleotides 49 to 58, 65 to 71 and 78 to 88 of the non-coding strand.

Fitting the zinc-fingers of TFIIIA within the proposed binding site

Over the last few years, three-dimensional structures of the zinc-finger motif have been elucidated both in solution and in complex with DNA. NMR studies on a number of peptides have shown that the zinc-finger motif has a general architecture, consisting of a two stranded β-sheet packed against an α-helix. A zinc ion is tetrahedrally co-ordinated by the pair of cysteines located in the β-sheet and the pair of histidines at the C-terminus of the α-helix (20–23). The crystal structure of a peptide containing the three zinc-fingers of the transcription factor Zif268 bound to 10 bp of DNA (3) provides the only example to date of how

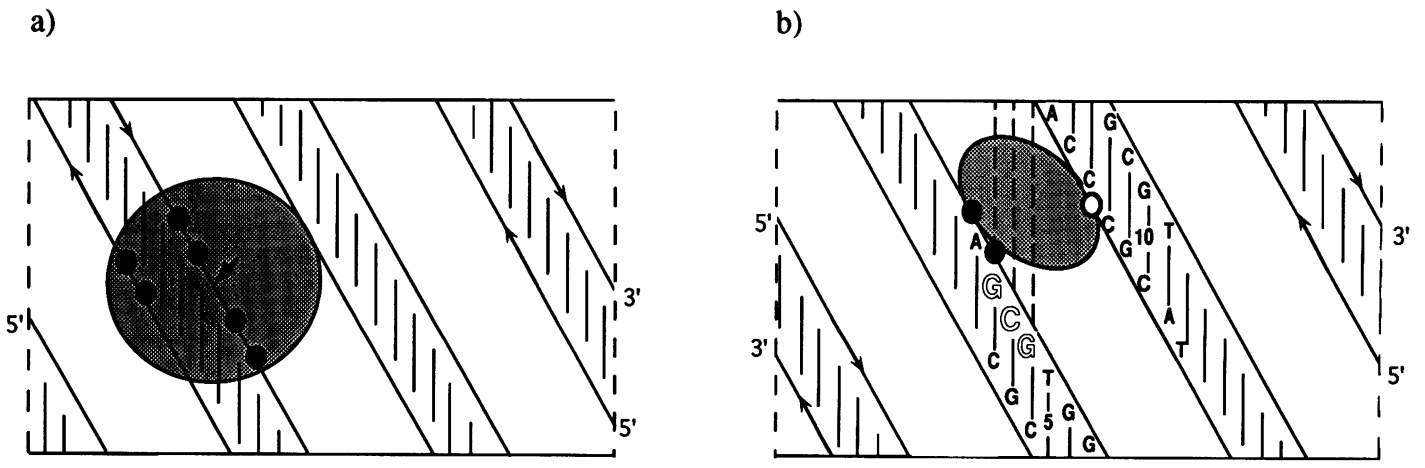

Figure 1. Schematic representation of the contacts made by the nuclease DNase I and a single zinc-finger domain with DNA. The contacts are in each case plotted on a cylindrical projection of a DNA double helix. The base pairs are drawn across the minor groove. In each case the grey shaded area represents the approximate diameter of (a) DNase I and (b) a zinc-finger (it is not meant to accurately represent the projected three-dimensional shape of the protein). Part (a) shows the phosphate contacts made by DNase I at a cleavage site, taken from the structure of the DNase I/DNA complex (1, 2). An arrow (↓) marks the DNase I cleavage site. The filled spots (●) indicate the phosphate groups contacted by DNase I to cleave at the site indicated. Part (b) shows the contacts made by a zinc-finger to DNA in the structure of the Zif268/DNA complex (3). The filled spots (●) indicate the phosphate groups involved in the binding of a zinc-finger. The unfilled spot (○) indicates a point of contact with the phosphate of the second strand of DNA which is found in one of the fingers. The bases shown in outline are the potential three base contacts. The base pairs are shown conventionally crossing the minor groove, but since the zinc-finger binds in the major groove the base pairs in its binding site are also represented in the major groove (dashed lines).

zinc-fingers interact with DNA in a sequence specific manner. In this complex the three fingers wind continuously around in the major groove for almost a complete turn of the double helix, making equivalent contacts to only one of the two DNA strands. The fingers bind in an anti-parallel fashion to this strand. The arrangement of the Zif268 zinc-fingers is topologically equivalent to model I described above. The binding sites of adjacent zinc-fingers overlap, so that the binding site for one finger spans four bases and the phosphate 5′ to the first base (Figure 1b). The details of this structure possibly reveal a general mechanism for sequence-specific recognition in which there are three main positions in the protein sequence involved in making contacts to a base triplet.

In the Zif268-DNA structure adjacent finger domains do not interact with each other and the linkers are extended with no significant DNA contacts, so that the orientation of adjacent fingers to each other seems determined solely by the way each interacts with DNA. The independence of finger domains joined by a flexible linker has also been observed in the NMR structure of a two finger peptide from the yeast transcription factor SWI5 (24, 25). Another case however, that of a two zinc finger peptide from the human enhancer binding protein MBP-1, shows that adjacent fingers may have a weak interaction between them (26). In conclusion, the structural information suggests that the way in which finger domains interact with DNA is likely to be conserved for the majority of zinc-fingers, but the orientation of one finger domain to its neighbour is likely to be dependent on the nature of the linker sequence and the organisation of the DNA sequence of the binding site.

The interpretation of the DNase I footprint of TFIIIA using the structure of the DNase I/DNA complex shows that the amount of DNA available for binding is much smaller than was presumed (4) and that it is divided into three areas: nucleotides 78 to 88, 65 to 71 and 49 to 58 as numbered on the non-coding strand (Figure 2). Thus, the possible options for fitting the nine fingers onto the binding site are greatly reduced. It can immediately be seen that it is not possible for all nine fingers to follow each other in the major groove, making specific contacts to three bases on the same strand, as seen in the Zif268/DNA complex. The protein must cross the minor groove twice, in the region of base pairs 78 and 65. Figure 3 shows schematically how the nine zinc-fingers of TFIIIA can be fitted onto the DNA binding regions defined by the DNase I cleavages in the complex. This arrangement takes into account the size of the binding site of a Zif268 zinc-finger, as described above, and the results from footprinting experiments for truncated forms of TFIIIA, as described below. The orientation of the protein on the DNA is 'anti-parallel' so that finger 9 binds to the 5′ end of the binding site and finger 1 to the 3′ end (7, 27).

Starting at the 3′ side of the binding site for TFIIIA the first patch of possible protein contact spans 11 bp, nucleotides 88 to 78. A peptide containing fingers 1, 2 and 3 has been shown to produce a DNase I footprint which is identical to the footprint of the whole protein in the region of nucleotides 76 to 96 of the non-coding strand. This shows that the first three fingers account for the TFIIIA-DNA interactions in this region (28, 29). Hence, in this alignment fingers 1 to 3 are shown binding successively in the major groove making contacts to nucleotides 78 to 88. The two linkers between these fingers have a sequence of TGEKP (or a slight variant) and are the same or very similar to those present in Zif268, adding support for a similar mode of binding for the first three fingers of TFIIIA.

After finger 3, TFIIIA would have to cross the minor groove at around nucleotide 78. This could be achieved by using the linker between fingers 3 and 4. There are two features of the protein sequence which favour the crossing of the minor groove by this linker: the linker between fingers 3 and 4 is one amino acid longer than usual and finger 3 has four amino acids between the pair of histidines, which is likely to distort the helix in that region, as has been observed in the NMR structure of a zinc-finger from the human protein ZFY (30). This could result in a change of direction for the exit of the peptide chain from this finger domain. Kochoyan *et al.* have also proposed that the linker between fingers 3 and 4 is used for crossing the minor groove (30).

The next and middle patch of contact is rather short, 7 bp, and spans nucleotides 71 to 65. Hydroxyl radical footprinting studies indicate that a peptide containing fingers 1 to 5 protects nucleotides 65 to 98 of the non-coding strand and 66 to 95 of

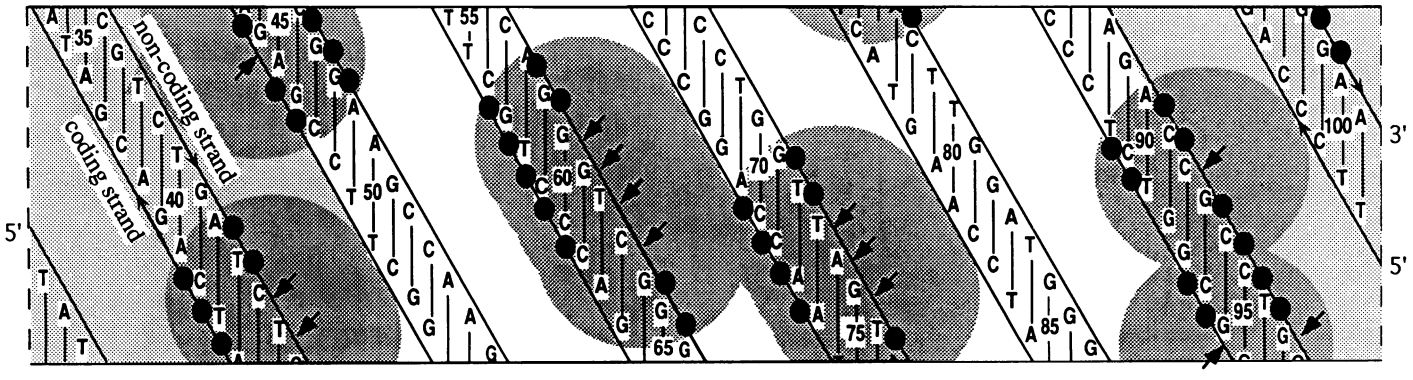

Figure 2. Plot of the DNase I cleavage sites for the TFIIIA/DNA complex. The sites of exposure to DNase I in the TFIIIA/DNA complex are plotted on a cylindrical projection of a DNA double helix. The base pairs are drawn across the minor groove. Arrows (↓) mark DNase I cutting sites. The filled spots (●) indicate the phosphates that are contacted by DNase I in order to cut the DNA, and hence are regions where DNA is accessible and not bound by TFIIIA. The dark grey shaded areas represent the area covered by DNase I in order to cut at the plotted cleavage sites. The areas were defined by overlapping DNase I binding sites as described in Figure 1a. The lighter grey represents exposure to DNase I outside of the immediate vicinity of the TFIIIA binding site. Thus the unshaded regions represent the DNA that is available for TFIIIA binding. There are very weak DNase I cleavages on the coding strand (not shown), the bonds between nucleotides 52 and 53, 67 and 68, and 70 and 71 (15). The cut between nucleotides 70 and 71 fits well with the proposed arrangement of fingers (Figure 3) whereas the others cannot be easily explained. These may arise because the fingers of TFIIIA bind weakly in these regions and can be displaced by DNase I.

the coding strand (27, 31). Therefore, it seems likely that fingers 4 and 5 account for the DNase I footprint in the region of nucleotides 66 to 71.

The protein must cross the minor groove again, around nucleotide 65. The linker between fingers 5 and 6 is particularly short and finger 6 shows the largest departure from the consensus sequence for zinc-fingers of all the nine present in TFIIIA. It would seem likely that finger 6 is being used in a different manner from the others and that it spans, and perhaps interacts in, the minor groove. This idea is also consistent with the fact that the linker following finger 6 is anomalously short.

The last patch of possible contact spans 10 bp, from nucleotide 58 to 49, which is just the right size to accommodate the last three fingers, 7, 8 and 9. It has been shown that TFIIIA truncated after finger 9, i.e. at the end of the complete zinc finger region, protects nucleotides 48 to 98 of the non-coding strand and nucleotides 45 to 95 of the coding strand (27, 31) (with virtually the same protection pattern as the whole intact protein). Therefore by analogy with the first three fingers, fingers 7, 8 and 9 are likely to bind successively in the major groove of the patch of contact spanning the 11 nucleotides from 49 to 58.

The consequence of this arrangement for the zinc-fingers of TFIIIA, in which some fingers bind consecutively in the major groove and the minor groove is crossed twice, is that TFIIIA, as a whole, binds to one side of the DNA double helix as proposed previously (4, 15, 16). This arrangement for the interaction of TFIIIA with DNA shows many of the features of the Zif268/DNA complex, yet resolves the topological problem that would arise if a protein with more than three zinc-fingers wrapped continuously around the DNA double helix. Since TFIIIA binds within the 5S RNA gene this would also facilitate the displacement of the protein upon transcription of the gene.

DISCUSSION

In this paper we describe how the precise information on the binding site for DNase I derived from the structure of the DNase I/DNA complex (1, 2) can be used to reinterpret the DNase I footprinting data for the TFIIIA/DNA complex. This approach for interpreting DNase I footprinting data is generally applicable to DNase I footprinting data from other DNA binding proteins and permits a more precise definition of the binding site for a protein. The method is essentially a simple two-dimensional approach for understanding a three-dimensional problem. It is somewhat limited in that DNase I is a large protein which binds essentially to the surface of the DNA double helix and sequence-specific DNA binding proteins tend to bind in the major groove of DNA, so that DNase I and a DNA binding protein could be seen to occupy the same two-dimensional space without occupying the same three-dimensional space. The main limitations are imposed by the inherent properties of footprinting data and are a consequence of the sequence specificity of DNase I. Since cleavage rates are affected by both the minor groove width and the flexibility of the DNA (1, 2, 32) and since these parameters can be affected by protein binding, it follows that the extent to which a footprint represents protein binding will vary with the protein/DNA complex studied. These limitations in the data have consequences on the application of the approach described here and may be overcome, in part, by making use of other footprinting reagents (4).

This new approach for the interpretation of DNase I footprinting data has been used in conjunction with the Zif268/DNA complex crystal structure (3) and data from footprinting experiments with truncated forms of TFIIIA to propose an arrangement for the nine zinc-fingers of TFIIIA to bind to DNA. The validity of the arrangement proposed for the zinc-fingers of TFIIIA has been examined with reference to the other available published footprinting data. It agrees well with hydroxyl radical footprinting, micrococcal nuclease footprinting, methylation interference, methylation protection and cross-linking experiments. If Figure 3 is compared with Figure 3 of Churchill *et al.* (16) it can be seen that the area of exposure to the hydroxyl radical agrees remarkably well to the area of DNA not bound by TFIIIA. The proposed arrangement of zinc-fingers also agrees with micrococcal nuclease footprinting experiments (4), taking into account the mode of action of this enzyme (33). Cross-linking experiments have identified a peptide corresponding to finger 2 and the linker between fingers 2 and 3 that can be cross-linked to nucleotide 84 of the non-coding strand (34) and in the alignment in Figure 3, finger 2 is in a suitable position to be cross-linked

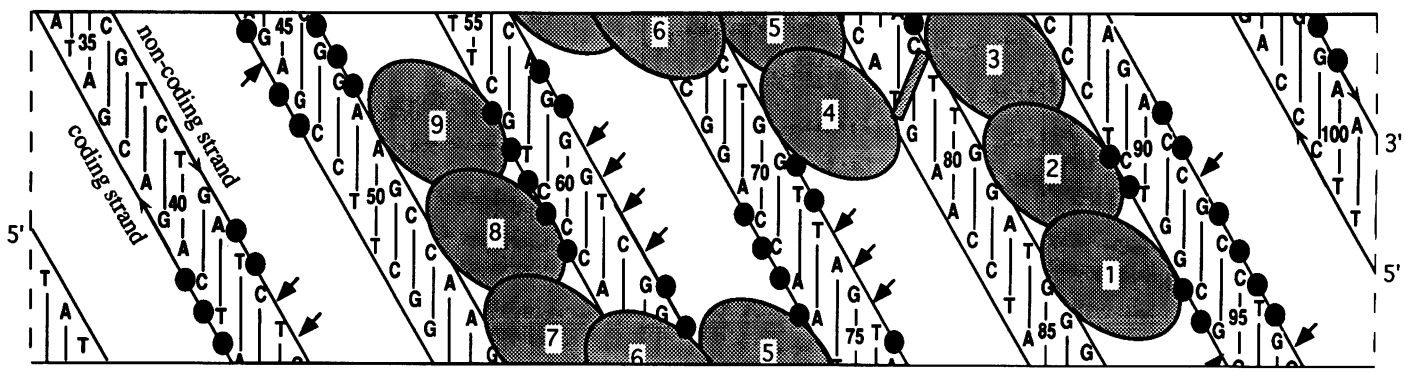

Figure 3. Schematic representation of the arrangement of the nine zinc-fingers of TFIIIA on the internal control region of the 5S RNA gene superimposed on the DNase I footprint. The sites of exposure to DNase I in the TFIIIA/DNA complex are plotted on a cylindrical projection of a DNA double helix. The base pairs are drawn across the minor groove. Arrows (↓) mark DNase I cutting sites. The filled spots (●) indicate the phosphates that are contacted by DNase I in order to cut the DNA, and hence are regions where DNA is accessible and not bound by TFIIIA. The nine zinc-fingers of TFIIIA have been fitted onto the three patches of available DNA and are shown as grey shaded areas (see Figure 1b). The grey shaded rectangle corresponds to the linker between fingers 3 and 4 crossing the minor groove.

to nucleotide 84. Experiments in which the protein was bound to methylated DNA showed that methylation of guanines 70, 71, 81, 82, 85, 86, 87 and 89 of the non-coding strand and 91 of the coding strand, which are located within the regions of DNA assigned to fingers, interfered with binding of TFIIIA (19). The arrangement proposed in Figure 3 is also consistent with most, but not all, of the methylation protection data (4). The observed protection of guanines 59, 60 and 61 on the non-coding strand appears to be in disagreement with the position of the fingers. However, it is important to remember that protection against such reagents may arise not only through protection by protein, but also through changes in DNA structure. A change, or distortion of the DNA structure in this region upon TFIIIA binding is also indicated by the marked change in the DNase I cleavage rate of the bonds between nucleotides 60 to 63 of the non-coding strand: in the protein/DNA complex these bonds are cut very rapidly, whereas in the naked DNA there is no cleavage {see Figure 2 of reference (15)}.

Although the two groups of three fingers, 1–3 and 7–9, are shown in our proposal to bind in a similar manner, there must be differences in their local interactions with the DNA. Deletion analyses of both the DNA binding site (35, 36) and TFIIIA (27), as well as methylation protection and interference experiments (4, 19), all show a polarity in the binding strength of the zinc-fingers of TFIIIA. Fingers 1–3 bind much more strongly than fingers 7–9. This difference in binding is also reflected by the different extent of protection offered by these two groups of fingers from the hydroxyl radical (16).

Thus all the combined data fits well with the alignment presented in Figure 3, but the main strength of this arrangement is that it is derived from data regarding the exposure of DNA to DNase I cleavage, the requirements for which are well understood. The binding sites for the enzyme cannot be occupied by another protein and thus the binding site of TFIIIA can be defined very precisely, leaving little choice for the disposition of the nine zinc-fingers of TFIIIA. The arrangement of the zinc-fingers deduced incorporates features of both the previously proposed models I and II (4): model I in that short runs of fingers wrap around the double helix in the major groove and model II in that the minor groove is crossed twice.

ACKNOWLEDGEMENTS

We would like to thank Aaron Klug and John Schwabe for their support, enthusiasm and comments on this manuscript.

REFERENCES

1. Suck, D., Lahm, A. and Oefner, C. (1988) Nature **332**, 464–468.
2. Lahm, A. and Suck, D. (1991) J. Mol. Biol. **222**, 645–667.
3. Pavletich, N. P. and Pabo, C. O. (1991) Science **252**, 809–817.
4. Fairall, L., Rhodes, D. and Klug, A. (1986) J. Mol. Biol. **192**, 577–591.
5. Miller, J., McLachlan, A. D. and Klug, A. (1985) EMBO J **4**, 1609–1614.
6. Jacobs, G. H. (1992) EMBO J. In press.
7. Smith, D. R., Jackson, I. J. and Brown, D. D. (1984) Cell **37**, 645–652.
8. Kadonaga, J. T., Carner, K.R., Masiarz, F.R. and Tjian, R. (1987) Cell **51**, 1079–1090.
9. Nagai, K., Nakaseko, Y., Nasmyth, K. and Rhodes, D. (1988) Nature **332**, 284–286.
10. Nardelli, J., Gibson, T. J., Vesque, C. and Charnay, P. (1991) Nature **349**, 175–178.
11. Sakaguchi, K., Appella, E., Omichinski, J. G., Clore, G. M. and Gronenborn, A. M. (1991) J. Biol. Chem. **266**, 7306–7311.
12. Thukral, S. K., Eisen, A. and Young, E. T. (1991) Mol. Cell. Biol. **11**, 1566–1577.
13. Fairall, L., Harrison, S. D., Travers, A. A. and Rhodes, D. (1992) J. Mol. Biol. **226**, 349–366.
14. Rhodes, D. and Klug, A. (1986) Cell **46**, 123–132.
15. Rhodes, D. (1985) The EMBO Journal **4**, 3473–3482.
16. Churchill, M. E. A., Tullius, T. D. and Klug, A. (1990) Proc. Natl. Acad. Sci. **87**, 5528–5532.
17. Berg, J. M. (1990) Annu. Rev. Biophys. Biophys. Chem. **19**, 405–421.
18. Pelham, H. R. B. and Brown, D. D. (1980) Proc. Natl. Acad. Sci. USA. **77**, 4170–4174.
19. Sakonju, S. and Brown, D. D. (1982) Cell **31**, 395–405.
20. Lee, M. S., Gippert, G. P., Soman, K. V., Case, D. A. and Wright, P. E. (1989) Science **245**, 635–637.
21. Klevit, R. E., Herriott, J. R. and Horvath, S. J. (1990) Proteins **7**, 215–226.
22. Omichinski, J. G., Clore, G. M., Appella, E., Sakaguchi, K. and Gronenborn, A. M. (1990) Biochemistry **29**, 9324–9334.
23. Neuhaus, D., Nakaseko, Y., Schwabe, J. W. R. and Klug, A. (1992) J. Mol. Biol. In press.
24. Neuhaus, D., Nakaseko, Y., Nagai, K. and Klug, A. (1990) FEBS Letters **262**, 179–184.
25. Nakaseko, Y., Neuhaus, D., Klug, A. and Rhodes, D. (1992) J. Mol. Biol. In press.
26. Omichinski, J. G., Clore, G. M., Robien, M., Sakaguchi, K., Appella, E. and Gronenborn, A. M. (1992) Biochemistry **31**, 3907–3917.
27. Vrana, K. E., Churchill, M. E. A., Tullius, T. D. and Brown, D. D. (1988) Mol. Cell. Biol. **8**, 1684–1696.
28. Christensen, J. H., Hansen, P. K., Lillelund, O. and Thogersen, H. C. (1991) FEBS Let. **281**, 181–184.
29. Liao, X., Clemens, K. R., Tennant, L., Wright, P. E. and Gottesfeld, J. M. (1992) J. Mol. Biol. **223**, 857–871.
30. Kochoyan, M., Havel, T. F., Nguyen, D. T., Dahl, C. E., Keutmann, H. T. and Weiss, M. A. (1991) Biochemistry **30**, 3371–3386.
31. Churchill, M. E. A. (1987) Ph. D. Thesis, Johns Hopkins University.
32. Drew, H. R. and Travers, A. A. (1984) Cell **37**, 491–502.
33. Cockell, M., Rhodes, D. and Klug, A. (1983) J. Mol. Biol. **170**, 423–446.
34. Lee, D. K., Evans, R. K., Blanco, J., Gottesfeld, J. and Johnson, J. D. (1991) J. Biol. Chem. **266**, 16478–16484.
35. Sakonju, S., Bogenhagen, D. F. and Brown, D. D. (1980) Cell **19**, 13–25.
36. Bogenhagen, D. F., Sakonju, S. and Brown, D. D. (1980) Cell **19**, 27–35.